*Earthquake Geotechnical Engineering for Protection and Development of Environment and Constructions – Silvestri & Moraci (Eds)*
*© 2019 Associazione Geotecnica Italiana, Rome, Italy, ISBN 978-0-367-14328-2*

# Serviceability of soil nailed walls in dynamic centrifuge tests

A. Ghadamgahi & M.H. Baziar
*Iran University of Science and Technology, Tehran, Iran*

A.J. Brennan
*University of Dundee, Dundee, UK*

ABSTRACT: Studies of seismic response of reinforced soil systems have largely focused on failure mechanisms. However, design requires demonstration that deformations are tolerable. To investigate the serviceability of a soil nailed wall, a centrifuge testing program was conducted. Model walls were constructed, and then subjected to three successive earthquake motions to determine their deformation under seismic loading. Models represented a prototype excavation of a 12 m deep wall with five rows of nails at a scale factor of 50. This paper summarizes the scaling considerations, the model preparation procedure and the method used to perform the tests. In addition, the result of a test on the nailed wall is presented through which the pattern of wall deformation and changes in the tensile load of an instrumented nail during the earthquake motions are reported and discussed.

## 1 INTRODUCTION

Soil nailing is a soil reinforcement method for stabilizing slopes and excavation walls and have been largely used all over the world during past four decades. There are many research works investigating different aspects of soil nailed systems using centrifuge model tests under static conditions (e.g. Tei et al. 1998, Zhang et al. 2001, Deepa & Viswanadham 2009, Zhang et al. 2014). First observations about the performance of soil nailed structures during earthquakes were reported by Felio et al. (1990) following the 1989 Loma Prieta Earthquake in the San Francisco Bay area. It was reported that the observed soil nailed systems did not show any significant movements or other indications of distress. Tufenkjian & Vucetic (2000) conducted a centrifuge test program, later continued by a further series of centrifuge tests (Kocijan & Vucetic 2002) to evaluate the failure mechanism of a 7.6 m soil nailed wall under strong horizontal shaking. The failure mechanism was described in two phases. The first phase was identified when soil nailed models exhibited a noticeable increase in the movements at the bottom of the excavation, corresponding to pullout of the bottom-row nails. The second phase of failure corresponded to a total collapse of the model due to the large displacements. This phase required large amplitudes of horizontal accelerations to initiate considerable deformations of the model nailed soil mass, showing that real scale soil nailed systems should be stable during strong earthquakes. However, for more reliable design methods of soil nailed walls in earthquake regions, investigating the serviceability of this retaining walls under real earthquakes is necessary. To measure seismically induced deformations in model walls, a centrifuge testing program was designed. The main testing procedure was established to investigate the effect of the following parameters on the soil nailed wall system under dynamic condition: 1- position of overburden pressure, 2- amount of overburden pressure and, 3- the length of the nails. This paper aims to present a description of the models, testing procedure and related testing limitations. Furthermore, the result of a test, test No. 1, including wall lateral displacements and tensile load changes along a soil nail, during three successive earthquake motions is presented.

## 2 CENTRIFUGE TESTS

### 2.1 *Test equipment*

The centrifuge test program was carried out at 50g utilizing the 3.5-m-radius beam centrifuge at University of Dundee, United Kingdom. This centrifuge was equipped with an Actidyn Q67–2 earthquake simulator (EQS). Brennan et al. (2014) has reported a detailed description about this facility. In the present study, an equivalent shear beam (ESB) container having interior dimensions of 675 mm in length, 280 mm in width and 334 mm in height was used. This container is composed of six solid aluminum frames that sandwich rubber layers to give similar dynamic shear stiffness as the surrounding soil and thereby decrease potential boundary effects attributable to the shear-wave reflection at the container walls. The design of this container can be found in Bertalot (2012).

### 2.2 *Model description and instrumentation*

Centrifuge modeling is a well-known physical modeling method which permits small-scale models to be tested under full-scale stress levels by applying increased gravitational acceleration. In centrifuge modelling of soil nailed walls, the equivalence of stresses and strains between the prototype and the model was considered as the reference to scale the characteristics of the problem. Centrifuge scaling relations are presented in Table 1. The scaling factor for all the test series was 50 which signifies that the dynamic centrifuge tests were carried out in-flight at a gravitational acceleration of 50 g. A typical layout of the model and its instrumentation is schematically shown in Figure 1. For the scaling factor $N$=50, a height of 240 mm for the model soil nailed wall corresponds to a prototype wall height of 12 m. The wall was reinforced with seventy-five 180-mm-long and 5-mm-diameter horizontal soil nails, arranged as five rows of seven at a spacing of 40 mm (2 m prototype). This was chosen to reflect the corresponding distance between the soil nails used in the construction of soil nailed walls in practice.

The model instrumentation shown in Figure 1 included linear variable differential transformers (LVDTs), miniature accelerometers (ACCs) and strain gages. The soil nailed wall system was instrumented with five LVDTs attached on a frame shown in Figure 2a designed to keep the LVDTs in right places. LVDTs 1 to 3 were positioned such that the lateral wall movements can be measured properly while LVDTs 4 and 5 were placed to monitor the vertical movements of the soil surface behind the facing. Once the model soil nailed wall had been constructed, the frame was installed on the container as shown in Figure 2b.

Three of the model soil nails were instrumented with strain gages as marked with a cross in Figure 1b. These nails were selected to investigate the distribution of axial tensile load along

Table 1. centrifuge scaling relations

| Quantity | Prototype | Model | Unit |
|---|---|---|---|
| Gravitational acceleration, g | 1 | N | $m/s^2$ |
| Stress, σ | 1 | 1 | Pa |
| Strain, ε | 1 | 1 | - |
| Linear dimension, L | 1 | 1/N | m |
| Area, A | 1 | $1/N^2$ | $m^2$ |
| Moment of Inertia, I | 1 | $1/N^4$ | $m^4$ |
| Displacement, δ | 1 | 1/N | m |
| Density, ρ | 1 | 1 | $kg/m^3$ |
| Young's modulus of elasticity, E | 1 | 1 | Pa |
| Axial stiffness, EA/L | 1 | 1/N | N/m |
| Flexural rigidity, EI | 1 | $1/N^4$ | $N.m^2$ |
| Force, F | 1 | $1/N^2$ | N |
| Acceleration, a | 1 | N | $m/s^2$ |
| Time (dynamic) | 1 | 1/N | s |

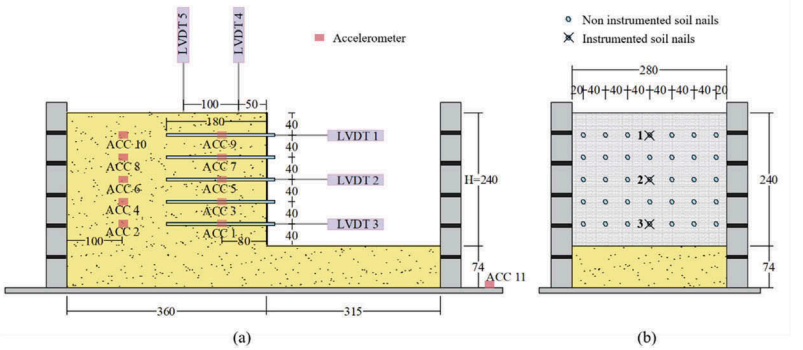


Figure 1. Centrifuge model layout and the instrumentation: (a) longitudinal cross section of model; (b) lateral cross section of model. All dimensions are in millimeters at model scale, scale factor = 50.

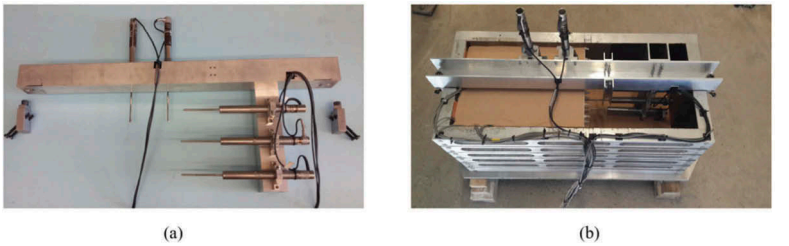


Figure 2. Model instrumentation with linear variable differential transformers: (a) frame for holding the LVDTs in right places; (b) Installed frame on the container

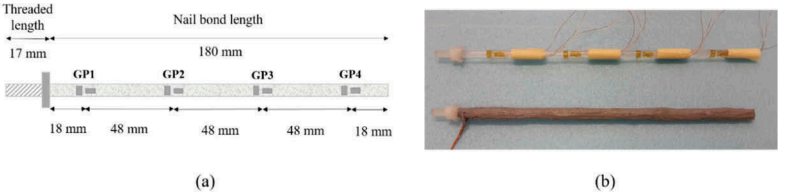


Figure 3. Soil nail instrumentation with strain gages: (a) schematic layout of strain gages along the rod; (b) instrumented soil nail before and after coating

the rods during earthquake motions when positioned at various elevation of the wall (stress levels). Figure 3a shows position of the strain gages along the instrumented soil nails. The soil nails were instrumented with four pairs of strain gauges wired in a half-bridge circuit to measure uniaxial strains along the bars throughout the process of applying earthquake motions.

A total number of eleven accelerometers were used for each test, ten of which were buried in the soil to measure the acceleration response at different altitudes during the earthquake motions and also to evaluate the dynamic soil properties (shear modulus and damping ratio) during earthquakes. The accelerometer No. 11 was installed on the base of container to govern the assigned acceleration excitation input.

### 2.3 *Soil properties*

The soil type, used in this study, was dry commercial HST 95, a uniformly-graded rounded silica sand. The basic properties of the soil material are shown in Table 2 (after Lauder 2010). The sand was placed into the container utilizing pluviation method (Ueno 2000). A target

Table 2. State-independent properties of HST95

| Property | Value |
|---|---|
| $D_{10}$ | 0.09 mm |
| $D_{30}$ | 0.12 mm |
| $D_{60}$ | 0.17 mm |
| Specific gravity, $G_s$ | 2.63 |
| Minimum void ratio, $e_{min}$ | 0.467 |
| Maximum void ratio, $e_{max}$ | 0.769 |

(Data from Lauder, 2010)

relative density of 60% was selected for all the centrifuge models which arrives the sandy soil at a medium dense state.

### 2.4 *Model soil nail and model facing*

Soil nails mainly work in tension, but they also mobilize stresses due to shear and bending at the intersection of the slip surface with the soil nails (Juran & Elias 1991, Lazarte et al. 2003). Under service load conditions, the contribution of shear stresses and bending moments of the nails is negligible (Jewell & Pedley 1990). In this study, it was assumed that mobilization of axial forces in the nails is the most significant aspect of the interaction between the soil and the nails. Accordingly, to select a proper material for the model soil nails, the main attention was given to the scaling of model nail axial stiffness. The selected material was then checked to satisfy the flexural rigidity scaling relation. The axial stiffness of the model and the prototype nails, $(EA/L)_{mn}$ and $(EA/L)_{pn}$, respectively, are related based on following equation:

$$\left(\frac{EA}{L}\right)_{mn} = \frac{1}{N}\left(\frac{EA}{L}\right)_{pn} \tag{1}$$

where $N$ is the model scale. On the other hand, the axial capacity of the prototype nail is assumed to be provided only by the axial capacity of the steel reinforcement. Thus, the equation 1 can be written as follows:

$$\left(\frac{EA}{L}\right)_{mn} = \frac{1}{N}\left(\frac{E_sA_s}{L}\right)_{pn} \tag{2}$$

where the model nail axial stiffness, $(EA/L)_{mn}$, is the product of the elasticity modulus and the cross-sectional area of the model nail, divided by its length. In a similar way, $(E_sA_s/L)_{pn}$ is the product of the elasticity modulus and the cross-sectional area of the prototype nail, divided by its length. Hence, required Young's modulus for the model soil nail can be derived from:

$$E_{mn} = \frac{1}{N}\left(\frac{E_sA_s}{L}\right)_{pn}\left(\frac{L}{A}\right)_{mn} \tag{3}$$

Nail length ratio (defined as the ratio between the nail length, $L$, and the wall height, $H$) has a common range of 0.5 to 1 in practice (Lazarte et al. 2003). As the model tests represented a soil nailed wall of 12 m high, considering a nail length ratio of 0.75, a length of 9 m for prototype soil nails corresponds to a model soil nail with 180 mm in length. For a 32 mm steel rebar with an elasticity modulus of $E_s$=2.1×10$^5$ MPa, assuming a diameter of 5 mm for model nails, the value of required elasticity modulus for model nail material was determined to be

$3.44\times10^3$ MPa. In this fashion, a model material closely matching this value can be selected. The selected material for the model nails, used in all the tests, was cast acrylic rods with an elasticity modulus of $3.3\times10^3$ MPa. This value corresponds to a small underestimation of the required elasticity modulus by 4%. Through scaling the axial stiffness, the scaling considerations with respect to the flexural rigidity were also satisfied. To simulate the soil-nail interaction, the soil nails required a fine coating of sand. This was applied by covering the bond length of the rods with a thin film of epoxy adhesive, and then rolling over them in the sand, to ensure that a smooth and uniform finishing was applied to each nail.

Lateral earth pressures acting against the facing produce flexural moments which means that the flexural capacity of the facing is a key factor in the design of soil nailed structures. In this study, the flexural rigidity per unit width of facing element is used as a dominant parameter to attain model facing characterizations. The thickness of model facing material can be obtained using the following relation:

$$t_{mf} = \frac{t_{pf}}{N}\sqrt[3]{\frac{E_{pf}}{E_{mf}}} \tag{4}$$

where $t_{mf}$ and $t_{pf}$ are the thickness of wall facing in model and prototype, respectively; $E_{mf}$ and $E_{pf}$ are the elasticity modulus of the facing material in the model and prototype, respectively. For a 140-mm-thick shotcrete facing assuming an elasticity modulus of $2.5\times10^4$ MPa, the required thickness of the model facing using aluminum material (elasticity modulus of $7\times10^4$ MPa), was calculated to be 1.99 mm. A 2-mm-thick aluminum sheet was selected for the model facing on which small diameter holes were drilled corresponding exactly to the location of each nail.

### 2.5 *Model preparation*

The construction of a soil nailed wall on a site is usually achieved using a step-by-step excavation process, drilling the boreholes, installation of the soil nails and then grouting. Modeling the real construction sequence while the centrifuge is in-flight is technically difficult and it was beyond the scope of this study. The principle used to prepare the model soil nailed wall is described here. Before the soil was pluviated into the container, a method for reduction of sidewall friction of the container was employed. As shown in Figure 4a, to minimize the effect of frictional resistance between the sidewalls of the container and the soil, the interior surfaces of the container were covered with strips of a low friction self-adhesive polytetrafluoroethylene (PTFE) tape having a thickness of 0.08 mm.

The sand was pluviated layer by layer into the container from a height of 1.2 m. The first layer was made by a thickness of 74 mm to achieve the level of the excavation subgrade. Following this, the aluminum facing was installed using temporary supports for holding it in the right place (Figure 4b). After installing the facing, the pluviation of the next soil layers and installation of the corresponding soil nails were performed step by step. During this process, once the desired thickness of soil for installing each row of the nails was achieved, pluviation of the sand was paused and the poured soil in the excavation area was vacuumed.

(a) (b)

Figure 4. Model preparation: (a) method used to reduce sidewall friction; (b) installed facing using temporary supports

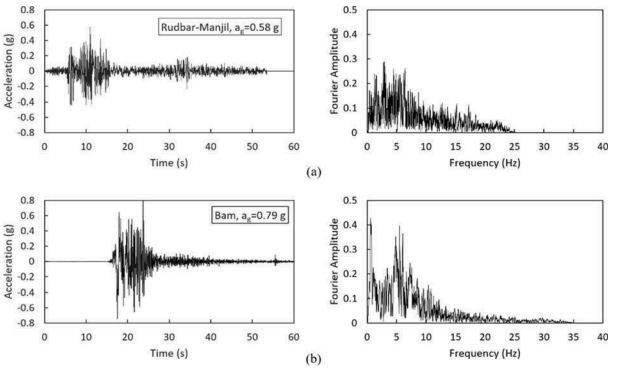


Figure 5. Reference ground motions: (a) Rudbar-Manjil earthquake; (b) Bam earthquake

Subsequently, seven soil nails for that level of deposited soil were horizontally installed through the holes of the retaining wall and head of the soil nails were assembled using a washer and a nut. During the process of soil nails installation at each level, the accelerometers were also buried at desired elevations (refer to Figure 1a).

### 2.6 *Testing procedure*

Following model completion, the model container was mounted onto the centrifuge for dynamic test. The model was spun up to a centrifugal acceleration of 50 g while all the measurements were recorded. Once the centrifuge had settled at 50 g, the model was subjected to three successive earthquake motions, with a short interruption, where the first and third earthquake inputs were identical. Data acquisition system was started to record all the measurements of the accelerometers, LVDTs and strain gages before applying each earthquake motion. The ground motion used as the first and third earthquakes was selected from the recorded motion at the Ab-bar station during the 1990 Rudbar-Manjil earthquake in Iran, having the moment magnitude of 7.4 and the peak ground acceleration of 0.58 g. The acceleration time histories of this record along with its Fourier amplitude spectra are illustrated in Figure 5a. The second earthquake input was selected from the recorded motion at the Bam station during the Bam earthquake in 2003, having the moment magnitude of 6.6 and the peak ground acceleration of 0.79 g. The acceleration time histories of Bam record and its Fourier amplitude spectra are shown in Figure 5b. To obtain demand input motions (those which were inputs as a target into the earthquake simulator), these two recorded motions were band-pass filtered between 0.8–8 Hz (40 – 400 Hz at model scale) utilizing a zero phase-shift digital filter to eliminate the signal components being outside the range that could be accurately controlled by the earthquake simulator. After filtering, the acceleration records corresponding to the time domain between 2-20 s (0.04-0.4 s at model scale) of Rudbar-Manjil earthquake and between 15-40 s (0.3-0.8 s at model scale) of Bam earthquake were selected to be used as the earthquake simulator inputs.

## 3 RESULTS

### 3.1 *Wall lateral displacement*

The response of soil nailed wall system to earthquake motions is shown in Figure 6. The results and values presented in this paper are quoted in prototype scale. Figure 6a indicates lateral displacements of the wall as a function of wall height. As is shown, the soil nailed wall system experienced a sharp lateral movement after first earthquake while the second and third motions caused a further moderate increase in the lateral wall deformations. The first motion gave rise to a lateral movement of 120 mm at the crest of the wall which increased by a quarter of this value after applying each of next two earthquake motions. The top of the wall moved more

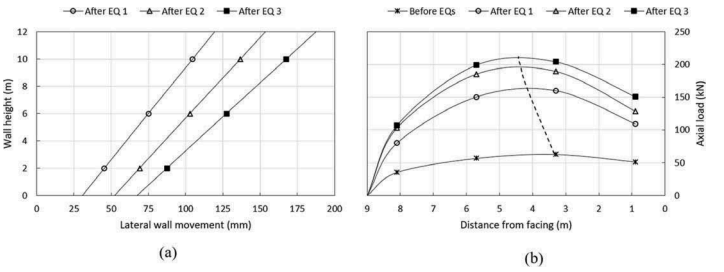


Figure 6. Response of soil nailed wall system to earthquake motions: (a) post-earthquakes lateral wall movements; (b) distribution of axial tensile load along soil nail 2 before and after applying earthquake motions

than the bottom after each earthquake motions, representing a rotation around the toe of the wall. This is consistent with those observations reported by Tufenkjian & Vucetic (2000).

### 3.2 *Distribution of tensile load along the soil nail*

The axial tensile load distribution along the instrumented rod in the middle of wall height (soil nail 2; see Figure 1b) before and after applying earthquake motions are shown in Figure 6b. As can be seen, the first earthquake led to a significant increase in the mobilized tensile load along the nail while the rate of increase in the axial load declined after each following earthquake. The value of maximum nail axial load ($T_{max}$) before applying earthquake motions was 63 kN, experiencing a significant increase of 99 kN after the first earthquake. However, this value increased by a further 31 kN and 16 kN due to the second and third earthquakes, respectively. The locus of $T_{max}$ before and after earthquakes are demonstrated with a dotted line in Figure 6b. As is shown, the location of peak axial load along the nail moved backward after applying each earthquake. The location of maximum tensile force in each soil nail occurs at interface between active and resistant zones (Phear et al. 2005). The resistant zone contains the length of the soil nails ($L_p$) which can develop pullout resistance and thereby contribute in the stability. Since the magnitude of $T_{max}$ and its location varied after applying earthquake motions, it can be concluded that the stability contribution of the middle soil nail changed due to earthquake motions. The resistant and active zones along the middle soil nail before and after earthquake motions are illustrated in Figure 7a-d where the resistant zone is schematically highlighted with a gray background. As shown in Figure 7a, b, the length of resistant

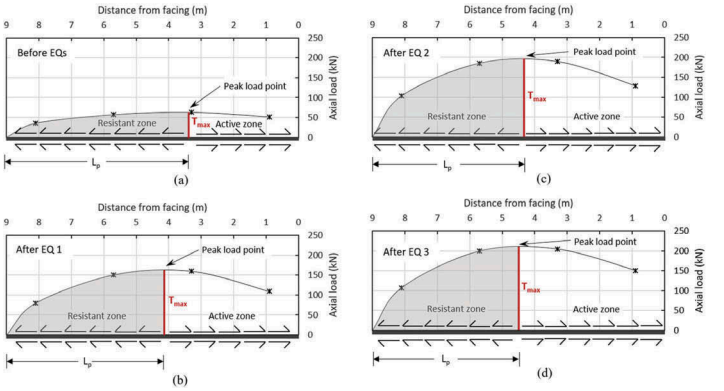


Figure 7. Illustrations of resistant and active zones along soil nail 2: (a) before applying earthquakes; (b) after earthquake 1; (c) after earthquake 2; (d) after earthquake 3

zone experienced a moderate decline after the first motion. However, due to the considerable rise in the magnitude of $T_{max}$, the stability contribution of the soil nail increased significantly after applying first earthquake motion. Figure 7b, c indicates that the length of resistant zone decreased slightly after second earthquake while the amount of $T_{max}$ experienced a further moderate increase which shows that more pull out resistance was developed along the resistant length after applying second earthquake. However, the third earthquake had a negligible effect on the magnitude of $T_{max}$ and $L_p$, as shown in Figure 7c, d, meaning that the stability contribution of the soil nail remained unchanged.

## 4 CONCLUSION

The focus of this paper was describing the centrifuge modeling procedure of a 12 m soil nailed wall. To achieve appropriate material for model soil nails and facing, the attention was given to the scaling of nail axial stiffness and flexural rigidity per unit width of the facing element, respectively. The model was constructed layer by layer using pluviation method. The model soil nailed wall was subjected to three successive earthquake motions where the first and third motions were identical. It was observed that the seismically induced wall deformations after first earthquake was significant compared with the following two earthquakes. The first earthquake mobilized a noticeable resistance along the resistant length of the soil nail located in the middle of wall height while the second earthquake gave rise to a further moderate increase in the nail tensile load. The stability contribution of the nail did not show a significant change after third earthquake.

## REFERENCES


Bertalot, D. (2012). Behavior of shallow foundations on layered soil deposits containing loose saturated sands during earthquakes. Ph.D. thesis, Univ. of Dundee, Dundee, U.K.

Brennan, A. J., Knappett, J. A., Bertalot, D., Loli, M., Anastasopoulos, I., & Brown, M. (2014). Dynamic centrifuge modelling facilities at the University of Dundee and their application to studying seismic case histories.

Deepa, V., & Viswanadham, B. V. S. (2009). Centrifuge model tests on soil-nailed slopes subjected to seepage. *Proceedings of the Institution of Civil Engineers-Ground Improvement*, 162(3),133–144.

Felio, G. Y., Vucetic, M., Hudson, M., Barar, O., & Chapman, R. (1990). Performance of soil nailed walls during the October 17, 1989 Loma Prieta Earthquake. *In Proceedings of the 43rd Canadian Geotechnical Conference, Quebec, Canada* (Vol. 1, pp. 165–173).

Jewell, R. A., & Pedley, M. J. (1990). Soil nailing design: the role of bending stiffness. *Ground Engineering*, 23(2).

Juran, I. and Elias, V. (1991). Ground Anchors and Soil Nails in Retaining Structures. *Foundation Engineering Handbook, Chap. 26, 2nd ed., Van Nostrand Reinhold, New York*, pp. 868–905.

Kocijan, J., & Vucetic, M. (2002). Organization and Interpretation of the Results of Dynamic Centrifuge Tests Conducted on 14 Models of Soil Nailed Walls. UCLA, the Henry Samueli School of Engineering and Applied Science.

Lauder, K. (2010). The performance of pipeline ploughs. Ph.D. thesis, Univ. of Dundee, Dundee, U.K.

Lazarte, C. A., Elias, V., Espinoza, R. D., & Sabatini, P. J. (2003). *Geotechnical engineering circular no. 7: Soil nail walls*. Federal Highway Administration, Washington, DC.

Phear, A., Dew, C., Ozsoy, B., Wharmby, N. J., Judge, J., & Barley, A. D. (2005). Soil nailing-best practice guidance (No. C637).

Tei, K., TAYLOR, N. R., & Milligan, G. W. (1998). Centrifuge model tests of nailed soil slopes. *Soils and foundations*, 38(2),165–177.

Tufenkjian, M. R., & Vucetic, M. (2000). Dynamic failure mechanism of soil-nailed excavation models in centrifuge. *Journal of Geotechnical and Geoenvironmental Engineering*, 126(3),227–235.

Ueno, K. (2000). Method for preparation of sand samples. *Centrifuge 98, T. Kimura, O. Kusakabe, and J. Takemura*, eds., Vol. 2, A.A. Balkema, Rotterdam, Netherlands. 1047–1055.

Zhang, G., Cao, J., & Wang, L. (2014). Failure behavior and mechanism of slopes reinforced using soil nail wall under various loading conditions. *Soils and Foundations*, 54(6),1175–1187.

Zhang, J., Pu, J., Zhang, M., & Qiu, T. (2001). Model tests by centrifuge of soil nail reinforcements. *Journal of testing and evaluation*, 29(4),315–328.